Supporting information for the article "Quantitative measurement of friction between single microspheres by friction force microscopy" by Xing Ling, Hans-Jürgen Butt, and Michael Kappl.

Improved procedure for determination the lateral calibration factor for friction force microscopy using the colloid probe technique

Among the several methods available for determining the lateral calibration factor, i.e. the factor to convert the lateral photodiode detector signal of the AFM to friction force, the one introduced by Ogletree *et al.*[1] might be most popular due to its relative ease of use and fair accuracy. However, the geometry of the faceted $SrTiO_3$ surfaces employed in this method limits it to cantilevers with AFM tips that have radii in the nanometer range. For colloid probes using micrometer-sized particles it is not applicable. Recently, Varenberg *et al.*[2] proposed an extension of the Ogletree method to any kind of AFM probe by using a wedge-shaped calibration grating. Such a grating is commercially available (TGF11 grating by MikroMasch, Tallinn, Estonia, cf. Figure 1). Its sloped facet has a width of ~2.2 µm, suitable for calibrating colloid probes with a tip diameter up to ~5.6 µm.

Varenberg *et al.*[2] derived equations from which the lateral calibration factor β (in N·m/V), as well as friction coefficient μ, can be calculated from the lateral cantilever deflection produced on the sloped facets during scanning. However, some imperfections were found in this method, which we shall address in the following to improve its accuracy.

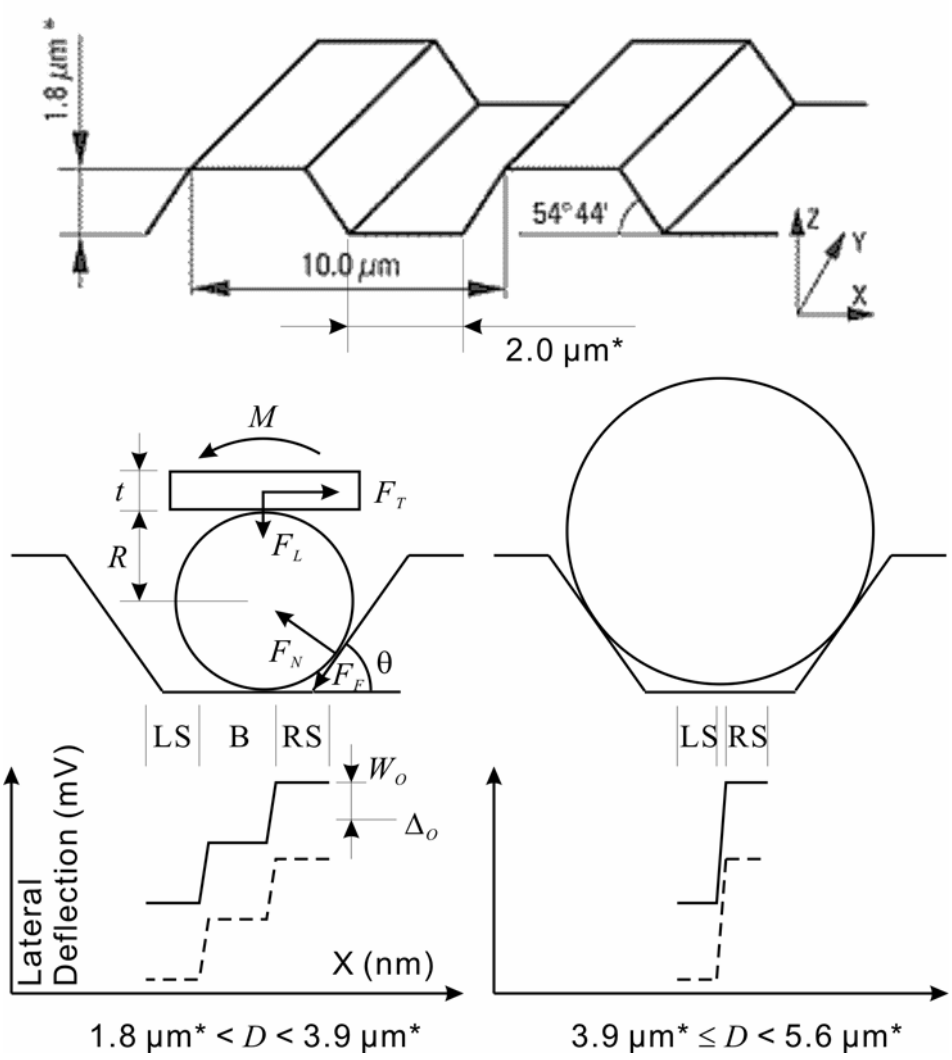

Figure 1. Top: dimensions of the TGF11 calibration grating. Middle: interaction geometry of the TGF11 grating with silica particles of different diameters attached to a tipless cantilever. Bottom: lateral deflection signals for sliding of a colloid probe on the grating surface. LS = left slope, RS = right slope and B = bottom, denote where the silica particle contacts the TGF11 grating.

The forces acting between the colloid probe and the facets of the grating are assumed to follow Amontons' law, i.e. $F_F = \mu\left(F_N + F_A^*\right)$, where F_A^* has the physical meaning of the adhesive force between tip and substrate and is referred to as effective

adhesion. F_F and F_N are lateral and normal force respectively; and μ is the friction coefficient. They must be balanced by load F_L, lateral force F_T, and torsion moment *M* applied by the cantilever (Figure 1). Varenberg *et al.* showed that this finally leads to a group of equations:[2]

$$\frac{\mu\left(F_L + F_A^* \cos\theta\right)}{\cos^2\theta - \mu^2 \sin^2\theta} = \frac{\beta W_o^0(M,\theta)}{R\left(1+\cos\theta\right)+t/2} \tag{1}$$

and

$$\frac{\mu^2 \sin\theta\left(F_L \cos\theta + F_A^*\right) + F_L \sin\theta\cos\theta}{\cos^2\theta - \mu^2 \sin^2\theta} - \frac{F_L R \sin\theta}{R\left(1+\cos\theta\right)+t/2} = \frac{\beta\Delta_o^0(M,\theta)}{R\left(1+\cos\theta\right)+t/2}. \tag{2}$$

Herein, the two unknown parameters β and μ are directly related to the measured lateral deflection quantities Δ_o and W_o, which are the offset and half-width between the trace and retrace signal on the sloped facets, respectively (Figure 1 bottom). Using V_{LD}^t and V_{LD}^r to denote the averaged trace and retrace lateral deflection, they are given by $\Delta_o = \left(V_{LD}^t + V_{LD}^r\right)/2$ and $W_o = \left(V_{LD}^t - V_{LD}^r\right)/2$. Solving the two above equations gives the values of β and μ. Therefore, an accurate determination of the parameters F_A^*, $\Delta_o^0(M,\theta)$, and $W_o^0(M,\theta)$ is necessary. According to our experiments, there were flaws in the former evaluations of these input parameters. First, a major source of error is the value of the effective adhesion F_A^*, which was suggested to be measurable as the pull-off force, which we found may not be applicable. A simple substitution of F_A^* with measured pull-off force can results in large errors in β and μ. Actually, Varenberg *et al.* had found that β and μ, which should be constant for a given setup, changed with load.[2] The authors did not clarify this unusual load-dependence, which we found reflects the error in determining F_A^*. Second, the detection of the cantilever deflection by the optical lever technique involves several contributions to the signal

measured. The torsional contributions of lateral deflection, $\Delta_o^0(M,\theta)$ and $W_o^0(M,\theta)$, need to be separated from the other sources to be inserted into the above equations to calculate β and μ. In our system, there are primarily three contributions: (1) Even without torsion moment, the lateral deflection of cantilever is not necessarily zero and requires compensation for a given load.[2] We also noticed that it slowly changes with time. (2) For samples of micrometer height variation, vertical deflection is may not remain constant during scanning due to the limited feedback response of the AFM. Such deviations will also change lateral deflection due to the coupling between vertical and lateral deflections. This deviation may be minimized by selection of experimental conditions. For instance, during the lateral calibration of cantilever, the scan rate was reduced to 0.4 Hz, which was sufficient to reduce the variation of vertical deflections to several millivolts. But for the scanning on particle surfaces with an increased rate of 1 Hz, the change of vertical deflection was observed to be up to 50 mV. This change and its effect on lateral deflection were considered for every individual data point. (3) Laser light passing besides or penetrating through the cantilever can reflect from the substrate and interfere with light reflected from the cantilever to create a background deflection signal, which changes with the relative height of cantilever to sample surface. Unfortunately, lateral deflection was found to be more susceptible to this interference than vertical deflection. To minimize this contribution an AFM with a short coherence IR laser diode was used. By this we were able to reduce the contribution of interference to the lateral deflection signal to below ~10 mV.

The different contributions to lateral deflection detector signal are summarized as

$$V_{LD} = V_{LD}^{0}(M) + V_{LD}^{\mathrm{I}}\left(V_{VD}^{\mathrm{Setpoint}}, \mathrm{time}\right) + V_{LD}^{\mathrm{II}}\left(V_{VD}^{\mathrm{error}}\right) + V_{LD}^{\mathrm{III}}(\mathrm{noise}),$$

where term V_{LD}^{0} denotes the contribution of torsion moment M (related to M by lateral calibration factor as $M = \beta V_{LD}^{0}$). The term $V_{LD}^{\mathrm{I}}\left(V_{VD}^{\mathrm{Setpoint}}, \mathrm{time}\right)$ denotes the static coupling between lateral and vertical deflection. The parameter of time reflects its drift. The term $V_{LD}^{\mathrm{II}}\left(V_{VD}^{\mathrm{error}}\right)$ denotes a dynamic coupling between lateral and vertical deflection. Any change of lateral deflection associated with the deviation of vertical deflection from setpoint is included in this term. The $V_{LD}^{\mathrm{III}}(\mathrm{noise})$ term is the noise floor of lateral deflection resulting from laser interference. With this description of lateral deflection, offset and half-width of the torsion loop are written as

$$\Delta_o = \Delta_o^0(M) + \Delta_o^{\mathrm{I}}\left(V_{VD}^{\mathrm{Setpoint}}, \mathrm{time}\right) + \Delta_o^{\mathrm{II}}\left(V_{VD}^{\mathrm{error}}\right) + \Delta_o^{\mathrm{III}}(\mathrm{noise}) \tag{3}$$

and

$$W_o = W_o^0(M) + W_o^{\mathrm{I}}\left(V_{VD}^{\mathrm{Setpoint}}, \mathrm{time}\right) + W_o^{\mathrm{II}}\left(V_{VD}^{\mathrm{error}}\right) + W_o^{\mathrm{III}}(\mathrm{noise}). \tag{4}$$

Only the zeroth terms Δ_o^0 and W_o^0 are connected to the torsion moment and should be separated from Δ_o and W_o. For lateral calibration, data were processed on a basis of individual AFM scan lines. Since at a scan rate of 0.4 Hz the deviation of vertical deflection from setpoint was negligible, the 2nd terms related to V_{VD}^{error} can be neglected. Also since the 1st and 3rd terms of lateral deflection do not depend on scan direction, from the definition of half-width of friction loop, the respective terms become zero, giving $W_o = W_o^0(M)$. Thus we only need to consider the 1st and 3rd terms for the offset of friction loop. According to the suggestion of Varenberg *et al.*, this can be done by combining the lateral deflection measured on flat surfaces. Since $\Delta_o^0(M)$ must be zero on flat surfaces, we obtain $\Delta_o(0) = \Delta_o^{\mathrm{I}}\left(V_{VD}^{\mathrm{Setpoint}}, \mathrm{time}, 0\right) + \Delta_o^{\mathrm{III}}(\mathrm{noise}, 0)$, where 0 indicates that the lateral deflection as measured on the flat part of the grating. Subtracting it from the offset

measured on sloped facet and recalling that $\Delta_o^{\mathrm{I}}\left(V_{VD}^{\mathrm{Setpoint}},\mathrm{time}\right)$ is a constant for the same scan line, $\Delta_o^0(M,\theta)$ can be expressed by $\Delta_o(\theta)-\Delta_o(0)$ with an error of $\Delta_o^{\mathrm{III}}(\mathrm{noise},0)-\Delta_o^{\mathrm{III}}(\mathrm{noise},\theta)$. Although the error was minimized to ~10 mV for our setup, it would introduce inaccuracy in the calculation of β and μ if we directly solve Equations 1 and 2, especially under small loads where the absolute value of $\Delta_o(\theta)-\Delta_o(0)$ is relatively small. Furthermore, as previously stated, there was an additional error in determining F_A^*. Ogletree *et al.* expressed similar concerns and suggested measuring friction loops under different loads and using their load dependence to avoid the uncertainty of determining F_A^* [1]. This strategy is also useful for colloid probes. By separating load F_L and effective adhesion F_A^*, Equations 1 and 2 can be rewritten as

$$W_o^0(M,\theta)=S_W F_L+I_W$$

and

$$\Delta_o^0(M,\theta)=S_\Delta F_L+I_\Delta,$$

where

$$S_W=\frac{R(1+\cos\theta)+t/2}{\beta}\frac{\mu}{\cos^2\theta-\mu^2\sin^2\theta} \tag{5}$$

$$I_W=\frac{R(1+\cos\theta)+t/2}{\beta}\frac{\mu\cos\theta}{\cos^2\theta-\mu^2\sin^2\theta}F_A^* \tag{6}$$

$$S_\Delta=\frac{R(1+\cos\theta)+t/2}{\beta}\frac{\mu^2\sin\theta\cos\theta+\sin\theta\cos\theta}{\cos^2\theta-\mu^2\sin^2\theta}-\frac{R\sin\theta}{\beta} \tag{7}$$

$$I_\Delta=\frac{R(1+\cos\theta)+t/2}{\beta}\frac{\mu^2\sin\theta}{\cos^2\theta-\mu^2\sin^2\theta}F_A^*, \tag{8}$$

The influence of F_A^* on lateral deflection is isolated to I_W and I_Δ. Besides, the error of determining $\Delta_o^0(M,\theta)$, $\Delta_o^{\mathrm{III}}(\mathrm{noise},\theta)-\Delta_o^{\mathrm{III}}(\mathrm{noise},0)$, is also separated into I_Δ since the noise is independent of load. Therefore, by linear fitting the plot of W_o and $\Delta_o(\theta)-\Delta_o(0)$ versus applied load, we can obtain precise values of S_W and S_Δ from the slopes. Substituting them into Equations 5 and 7 yields values of μ and β that should be consistent for data measured under different loads. They are used as references for calculating other quantities or for comparison. For example, from Equation 6, we can calculate the value of F_A^*. This allows the comparison with measured pull-off forces. Additionally, by dividing Equation 8 with Equation 6, a second value of μ is determined, that contains the error of $\Delta_o^{\mathrm{III}}(\mathrm{noise},\theta)-\Delta_o^{\mathrm{III}}(\mathrm{noise},0)$. The difference between this and the first value reflects the level of noise.

When the particle diameter exceeds 3.9 μm, the colloid probe cannot reach the planar bottom of the grating due to the limited distance between the sloped facets of the TGF11 grating (Figure 1). Scanning on the planar top of grating is inappropriate since the sharp edge of crest easily wears the colloid probe resulting in irregular lateral deflection. Therefore, we used an alternative method to determine $\Delta_o^{\mathrm{I}}\left(V_{VD}^{\mathrm{Setpoint}},\mathrm{time}\right)$ by scanning opposing slopes (Figure 1). From Figure 1, we know that $\Delta_o^0(M,\theta)=-\Delta_o^0(M,-\theta)$. By adding the offsets of torsion loops obtained on left slope and right slope and recalling that $\Delta_o^{\mathrm{I}}\left(V_{VD}^{\mathrm{Setpoint}},\mathrm{time}\right)$ is a constant for the same scan line, we obtain

$$\Delta_o^{\mathrm{I}}\left(V_{VD}^{\mathrm{Setpoint}},\mathrm{time},\theta\right)=\left(\Delta_o(\theta)+\Delta_o(-\theta)-\Delta_o^{\mathrm{III}}(\mathrm{noise},\theta)-\Delta_o^{\mathrm{III}}(\mathrm{noise},-\theta)\right)/2\,.$$

Thus $\Delta_o^0(M,\theta)$ can be expressed by $\left(\Delta_o(\theta)-\Delta_o(-\theta)\right)/2$ with an error of $-\left(\Delta_o^{\mathrm{III}}(\mathrm{noise},\theta)-\Delta_o^{\mathrm{III}}(\mathrm{noise},-\theta)\right)/2$. The error is also separated into I_Δ and the

Equations 5-8 can be directly used without any modification. For the smallest particle of 1.43-μm-radius we used both methods for determining $\Delta_o^0(M,\theta)$ obtaining comparable results.

Table 1 lists results of several calibration experiments using different probes. Values of β, μ, and F_A^* were calculated from Equations 5-8. Pull-off forces measured from force curves are also listed for comparison. The deviation of effective adhesion F_A^* from measured pull-off force F_A is obvious and the noise influence can be identified from the μ estimated from $I_\Delta \cot\theta / I_W$. Note that for the five cantilevers (1, 2, 3, 5, 6) showing similar normal spring constant and sensitivity, the lateral calibration factors are close to each other with a deviation of only ±10%.

Table 1. Results from the calibration procedure to determine the lateral calibration factor.

	Particle Radius (μm) ± 0.05	Normal Spring Constant (nN/nm) ± 0.5	Normal Sensitivity (mV/nm)	β (μN·nm /mV) ± 2	μ ± 0.02	$\frac{I_\Delta \cot\theta}{I_W}$ ± 0.02	F_A^* (nN) ± 50	Measured Adhesion F_A (nN)
1	1.67	17.8	34.6 ± 0.1	51	0.24	0.21	130	1030 ± 20
2	1.43	17.1	37.6 ± 0.3	54	0.23	0.29	1050	1200 ± 100
				55	0.24	0.19	1050	
3	1.67	17.8	35.9 ± 0.1	48	0.20	0.24	130	547 ± 7
4	2.10	28.3	37.0 ± 0.7	87	0.29	0.30	1460	980 ± 70
5	1.43	17.1	37.7 ± 1.1	53	0.22	0.16	670	250 ± 20
				51	0.22	0.21	670	
6	1.75	16.1	31.4 ± 0.7	59	0.22	0.15	1080	355 ± 9

Calibration results for 6 independent experiments using 4 different probes. All probes were calibrated using two oppositely sloped facets of the grating. For cantilevers with similar normal spring constant, we get a very close agreement of the lateral calibration factors. For the smallest particle of 1.43-μm-radius (2nd and 5th rows), the calibrations were carried out using the grating bottom and one sloped facet (first line) as well as opposing facets (second line). No significant difference is found for these two approaches.

References

1. Ogletree, D. F.; Carpick, R. W.; Salmeron, M. *Review Of Scientific Instruments* **1996,** 67 (9), 3298-3306.

2. Varenberg, M.; Etsion, I.; Halperin, G. *Review of Scientific Instruments* **2003,** 74 (7), 3362-3367.